JOURNAL OF APPLIED ELECTROCHEMISTRY 26 (1996) 1125–1132

Characterization of the efficiency of antiscale treatments of water
Part I: Chemical processes

C. GABRIELLI, M. KEDDAM, H. PERROT

Laboratoire de Physique des Liquides et Électrochimie UPR 15 CNRS, Tour 22, 4 Place Jussieu, 75252 Paris, Cedex 05, France

A. KHALIL, R. ROSSET, M. ZIDOUNE

Laboratoire de Chimie Analytique des processus Industriels URA CNRS no. 437, ESPCI, 10 rue Vauquelin, 75231 Paris, Cedex 05, France

Received 27 July 1995; revised 16 April 1996

The efficiency of chemical antiscale treatments was assessed by various techniques: chronoamperometry, electrogravimetry and impedance measurement. Electrogravimetry gave data directly readable by the user. The particular chemistry of the additives may give results more difficult to interpret through chronoamperometry, where the residual current often increases when the quantity of antiscale chemical species increases.

1. Introduction

Calcareous scale deposits from natural hard water supplies (especially hot waters) in industrial plants or domestic equipment lead to technical and economical problems [1, 2] such as (i) total or partial obstruction of pipes leading to a decrease in flow rate, (ii) reduced heat transfer as calcium carbonate scale is 15 to 30 times less conductive than steel, (iii) seizure of valves and (iv) clogging of filters.

In some nuclear power plants the power produced is limited by scaling in cooling towers which leads to overheating of the core (e.g., 500 tons of calcareous scale deposited on their surface, about 2.4 km^2, have been described). In Great Britain nonproduction expenses related to scaling have been estimated at 600 millions pounds per year to repair pipes, boilers, water-heaters, etc. damaged by scale.

Therefore, water treatment leading to calcium carbonate precipitation in bulk solution in such a way that the scales formed do not encrust the walls is desirable. Chemical and physico-chemical treatments have been employed to date. These prevent either the causes or the consequences of calcareous precipitation. For the causes, the ions responsible for scale formation are eliminated. For the consequences, as encrustation of $CaCO_3$ is considered as disastrous, it is necessary to delay nucleation phenomena or to favour homogeneous nucleation to the detriment of heterogeneous nucleation (i.e. to favour precipitation in bulk solution and not on walls).

The acceleration of scaling processes is convenient to estimate the efficiency of antiscale treatments. For this purpose electrochemical techniques were used here [3–5]. In this paper only the efficiency of chemical treatments were evaluated, the evaluation of the efficiency of the physico-chemical treatments will be reported in a companion paper [6].

Chemical treatments can be separated into two types: chemical processes, on the one hand, which need quantities of reagents proportional to the concentration of calcium ions in solution: for example, acid addition or lime decarbonation; scaling inhibitors, on the other hand, which work at very low concentration (often less than 1 mg dm^{-3}).

2. Experimental details

Accelerated scaling was carried out at ambient temperature by polarizing the electrode at potentials where electrochemical reduction of the oxygen dissolved in the tested water occurred according to [3–5]:

$$O_2 + 2H_2O + 4e^- \rightarrow 4OH^-$$

The production of OH^- ions led to an increase in pH near the electrode which allowed $CaCO_3$ to be precipitated as a solid phase (s) on the electrode according to the chemical reaction:

$$Ca^{2+} + HCO_3^- + OH^- \rightarrow CaCO_3\,(s) + H_2O$$

The calcareous deposit progressively covered the metallic electrode and isolated the metal from the solution. Consequently, the basic techniques used in this paper to estimate the efficiency of chemical treatments (and physical treatments in the following paper) consisted in measuring the change of either the current (chronoamperometry), the $CaCO_3$ mass (chronoelectrogravimetry) or the electrochemical impedance with respect to time during scaling while the electrode was polarized at the limiting current for oxygen reduction (ca. −1 V vs SSE). For chronoamperometry and

0021-891X

impedance measurements a platinum disc electrode, usually rotating at 1000 rpm, was used. For chronoelectrogravimetry, a gold electrode of a home made electrochemical quartz microbalance was employed. The electrochemical impedance was measured using a frequency response analyser (Solartron 1250). Fig. 1(a), (b) and (c) give examples of the three basic recordings where the main parameters which characterize scaling are defined.

2.1. *Chronoamperometry*

Figure 1(a) shows a chronoamperometric curve with its characteristic decreasing shape whose slope is related to the scaling rate [3–5]. Ledion [3] defined the scaling time, t_s, as the intersection of the tangent at the inflexion point of this curve and the time axis. The residual current i_{res} (beyond the scaling time) is related to the deposit morphology; the more compact and insulating the scale, the lower the residual current.

2.2. *Chronoelectrogravimetry*

By using a quartz microbalance it is now possible to continuously follow extremely tiny mass changes (Fig. 1(b)) [6–9]. The working electrode was fixed and either the solution was stirred or an impinging jet cell was used [8]. A quartz resonator with gold electrodes was inserted in an oscillator. The oscillation frequency change, Δf, is proportional to the mass of scale deposited. Δm, on the surface according to

$$\Delta f = -\frac{2f_o^2}{dvS}\Delta m$$

where f_o is the quartz resonance frequency, d, the quartz density, v, the speed of ultrasonic wave in the quartz and S, the active surface of the quartz.

Figure 1(b) shows a chronoelectrogravimetric curve which exhibits three steps in the scaling process: (i) during the first 10 to 25 min (see insert) the mass of scaling increased slowly; (ii) from 20 to 150 min the mass of scaling increased proportionally with time (i.e., with a constant rate); (iii) beyond 150 min the mass of scaling increased very slowly. This will be called the 'plateau' region later, even though the mass is still generally increasing slightly.

From this curve, several characteristic times can be defined:

t_N, the nucleation time corresponding to the end of the first stage. This is defined by the intersection of the linear part and the time axis.

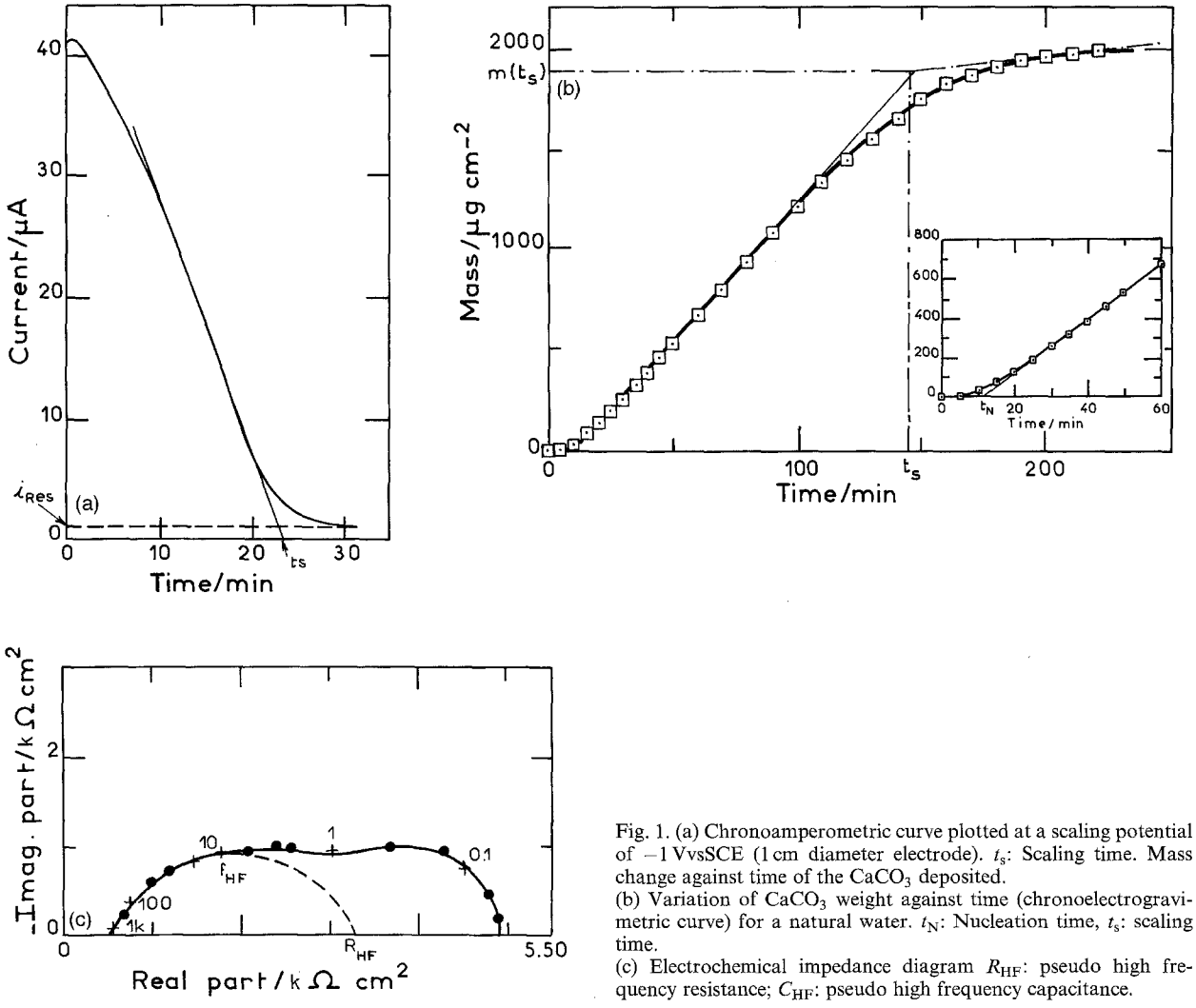

Fig. 1. (a) Chronoamperometric curve plotted at a scaling potential of −1 VvsSCE (1 cm diameter electrode). t_s: Scaling time. Mass change against time of the $CaCO_3$ deposited.
(b) Variation of $CaCO_3$ weight against time (chronoelectrogravimetric curve) for a natural water. t_N: Nucleation time, t_s: scaling time.
(c) Electrochemical impedance diagram R_{HF}: pseudo high frequency resistance; C_{HF}: pseudo high frequency capacitance.

V_S, the scaling rate corresponds to the slope of the intermediate linear part.
t_S, the scaling time corresponds to the end of the intermediate stage. It is defined by the intersection of the linear part and the plateau.
$m(t_S)$, the total deposited mass on the plateau.

2.3. *Electrochemical impedance*

During scaling process the measured impedance showed two time constants more or less well separated (Fig. 1(c)) [11–13]. It was demonstrated that the high frequency time constant allows a pseudo high frequency resistance R_{HF} and a pseudo high frequency capacitance C_{HF} to be defined which were related to the coverage rate of the scale [12, 13]. The low frequency time constant was related to the oxygen diffusion in the solution bulk.

In Fig. 1(c) R_{HF} and the pseudo characteristic frequency f_{HF} are indicated. C_{HF} is obtained from these values through $2\pi f_{HF} R_{HF} C_{HF} = 1$. A fitting procedure to a model, based on a simplex algorithm, was used to estimate R_{HF} and f_{HF}.

3. Chemical processes

The efficiency of two types of chemical processes were estimated: acid addition and lime decarbonation.

3.1. *Acid addition*

Calcium carbonate, which may lead to scaling from supersaturated $CaCO_3$, is present in the solution as Ca^{2+} and HCO_3^- ions. Acid addition, usually sulfuric acid, is often termed acid vaccination. It destroys the HCO_3^- ions according to

$$HCO_3^- + H^+ \rightarrow CO_2\,(g) + H_2O$$

The gaseous carbon dioxide CO_2(g) produced escapes to atmosphere which decreases the $CaCO_3$ deposition rate. $CaSO_4$, much more soluble ($\sim 2\,g\,dm^{-3}$) than $CaCO_3$, is not deposited under usual conditions.

Chronoamperometric curves were recorded for natural waters brought to various pH by acid addition (three tests for each pH value) (Fig. 2(a)). Measured scaling times were plotted against pH in Fig. 2(b). It was observed that t_S increased when pH decreased. Below pH 7 this increase was very sharp. At pH 6.25, scaling did not occur.

Chronoelectrogravimetric curves were recorded at various pH for scaling up to 80 min, that is, before the plateau was reached (Fig. 3(a)). Figure 3(b) shows the mass of $CaCO_3$ deposited after 80 min against pH. It decreases when pH decreased and tends to zero below pH 6.25. It was noticed that, at pH 6, there was no observable deposit on the electrode up to 30 min. These curves showed that the nucleation

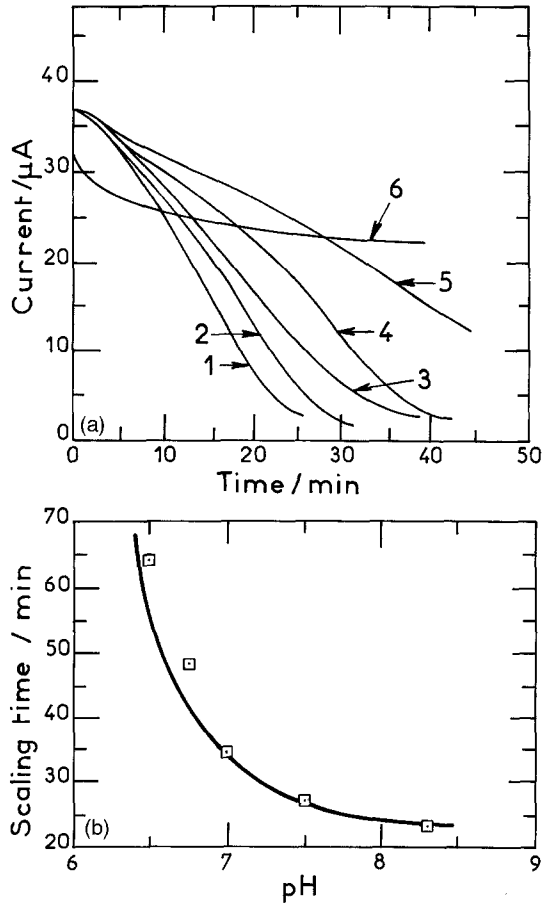

Fig. 2. (a) Chronoamperometric curves (2 mm diam. electrode) plotted at various pH: (1) 8.1, (2) 7.5, (3) 7.0, (4) 6.75, (5) 6.5 and (6) 6.25. (b) Change of the scaling time against pH from experiments of (a).

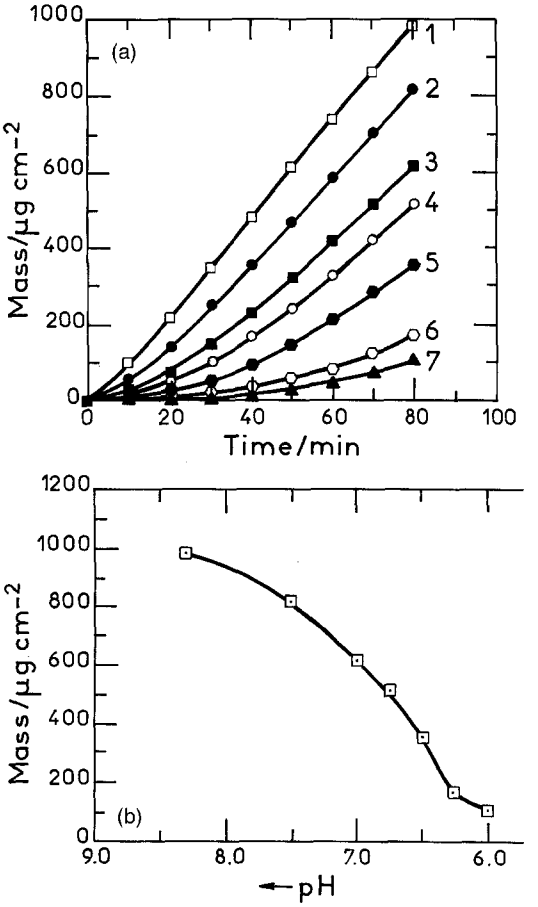

Fig. 3. (a) Chronoelectrogravimetric curves plotted at various pH: (1) 8.3, (2) 7.5, (3) 7.0, (4) 6.75, (5) 6.5, (6) 6.25 and (7) 6.0. (b) Change of the $CaCO_3$ mass deposited at 80 min, from experiments of (a).

time increased when the pH decreased. However, after some time the scaling rate seemed to be roughly pH independent.

Observation of $CaCO_3$ deposition at pH 6 is not in disagreement with thermodynamics. As dissolved oxygen is reduced to OH^- ions even in acid solution, the near electrode solution is more basic than the bulk and a strong pH gradient is established. Therefore, $CaCO_3$ precipitation may occur on the electrode.

Chronoamperometry and chronoelectrogravimetry demonstrated the efficiency, well known from a practical point of view, of the acid addition. These two techniques may allow the adaptation of the working conditions of equipment with respect to parameters like temperature, physico-chemical characteristics of waters, prevailing regulations about discharge of wastes to rivers, etc. This could be particularly useful for nuclear power plants, which consume large amounts of cooling water.

3.2. *Lime decarbonation*

For convenience and economic reasons, lime is the most common alkaline reactive used to add OH^- ions to natural waters. The chemical reactions which occur depend on whether the water is aggressive or calcifying:

(a) with an 'aggressive' water (where CO_2 is in excess), the first step is a neutralization according to

$$2CO_2 + Ca(OH)_2 \rightarrow Ca^{2+} + 2HCO_3^-$$

that is,

$$CO_2 + OH^- \rightarrow HCO_3^-$$

During this step there is a complete transformation of CO_2 to HCO_3^-. At the end of this neutralization of CO_2, the system can be considered as at equilibrium where it stays during the next step identical to the second case.

(b) with a water at equilibrium or slightly calcifying, $CaCO_3$ precipitates according to

$$Ca^{2+} + 2HCO_3^- + Ca(OH)_2 \rightarrow 2CaCO_3\,(s) + 2H_2O$$

Chronoamperometric curves were recorded during lime addition. Figure 4 shows the change of scaling time against Ca^{2+} concentration: Lime decarbonation has an appreciable effect for waters whose calcium concentration is lower than 100 mg dm^{-3}.

Chronoelectrogravimetric curves lead to results in agreement with the previous ones. When calcium concentration decreased the mass of deposited scale, after a given time, linearly decreased down to 120 mg dm^{-3} and then more slowly. When calcium concentration was less than 80 mg dm^{-3} the mass of scale deposited after 20 min was negligible (Fig. 5).

4. Scale inhibitors

Scale inhibitors work at very low concentration (often less than 1 mg dm^{-3}) by adsorption on the $CaCO_3$

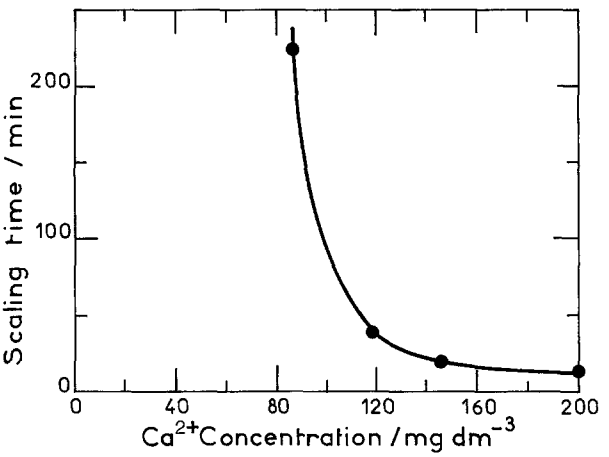

Fig. 4. Change of the scaling time at 20 °C obtained from chronoamperometric curves against Ca^{2+} concentrations of water decarbonated with lime.

nuclei. They provoke morphological changes which lead to nonadherent scale. Their action is very different from the chemical processes where calcium is complexed to avoid $CaCO_3$ precipitation. These processes need a quantity of reactive species proportional to the amount of calcium in solution. However, the use of scale inhibitors is not allowable in drinking water. They are used only for closed circuit equipment (e.g., heating systems), industrial installations when the quantity used (and wasted) are compatible with environment constraints and they are added to all domestic or industrial detergents (mainly phosphates, phosphonates and polycarboxylates).

The scale inhibitor family is very wide. Most of these products can be gathered in several groups with a common architecture which has antiscale properties. These include: orthophosphates and condensed phosphates, organo-phosphonates and polycarboxylates [14].

Some other additives are active in scale prevention: for example, filming fat amines with long chains are used for corrosion prevention but as they easily adsorb on metals they also sometimes have antiscaling properties.

Scaling can be prevented at two levels: nucleation and growth of the crystals and surface state of the walls.

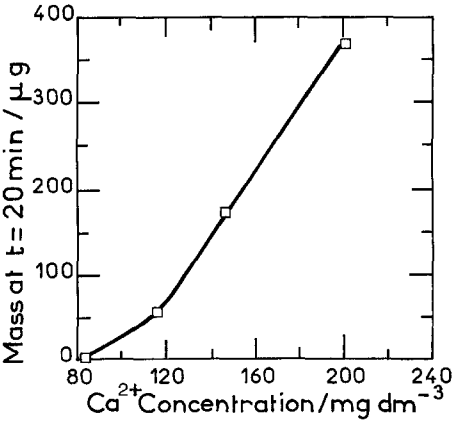

Fig. 5. Mass of scaling deposited after 20 min against the Ca^{2+} ions concentrations of water after lime decarbonation.

4.1. *Inorganic phosphates*

Inorganic phosphates can be classified in several categories [15]. These include: (i) simple phosphates, PO_4^{3-}; (ii) polyphosphates, linear groups of PO_4^{3-}; (iii) ultraphosphates, ramified groups of PO_4^{3-}; and (iv) metaphosphates, cyclic pattern of PO_4^{3-} groups.

Scaling inhibition was first demonstrated with these products (e.g., 1 to 10 ppm of sodium hexametaphosphate inhibit scale formation). However, a fast hydrolysis in orthophosphates, which have less antiscale effect, is the drawback of inorganic polyphosphates in water treatment.

Figure 6 shows chronoamperometric curves recorded when increasing quantities of dihydrogenophosphate $H_2PO_4^-$ were added to natural water. These curves show that, in the presence of orthophosphates, the current rapidly decreases to tend towards a residual current. However, the blocking of the electrode is not due to $CaCO_3$ deposition but to calcium hydrogenophosphate ($CaHPO_4$) precipitation in alkaline medium (between pH 7 and 8) according to

$$H_2PO_4^- + Ca^{2+} + OH^- \rightarrow CaHPO_4\,(s) + H_2O$$

Calcium was precipitated in the form of acid phosphate and the scaling time became infinite. When the $H_2PO_4^-$ concentration increased, the shape of the chronoamperometric curve changed; the scaling time became infinite but the residual current increased. However, the main point was that scaling was stopped.

4.2. *Organic phosphates*

The effect of a phosphonic acid: aminotris-(methylene-phosphonic) acid or ATMP (from Monsanto) was tested [15]. It has the form

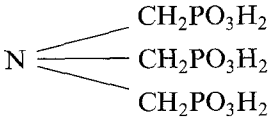

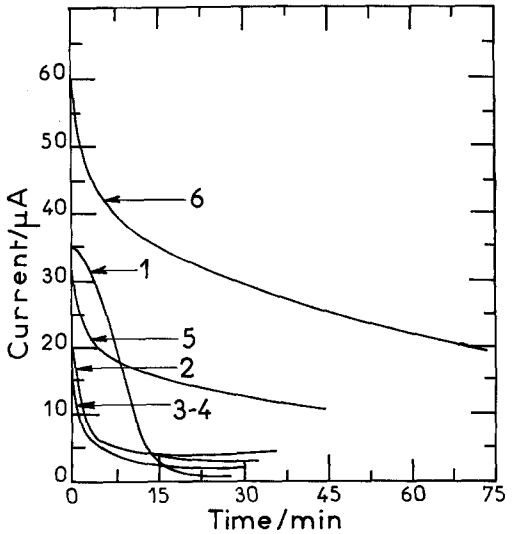

Fig. 6. Chronoamperometric curves plotted with various amount of KH_2PO_4 added to a natural water. (1) No addition; (2) 1×10^{-4}, (3) 5×10^{-4}, (4) 1×10^{-3}, (5) 5×10^{-3} and (6) 1×10^{-2} M.

Chronoamperometric curves were recorded for various ATMP amounts added to water with 100 mg dm^{-3} calcium concentration [16]. Figure 7(a) shows the scaling time, t_s, against ATMP concentration. It can be considered that beyond 0.5 mg dm^{-3}, t_s, became infinite: $CaCO_3$ did not adhere to the platinum electrode. Another representation of the phenomena is the plotting of the residual current against ATMP concentration (Fig. 7(b)), as this current measured the dissolved oxygen reduction rate at the electrode covered by a $CaCO_3$ deposit. The more compact and adherent the deposit is, the less oxygen can diffuse across this insulating film and the lower the residual current is. Figure 7(b) confirms that the $CaCO_3$ deposit starts limiting the oxygen reduction from 0.4 mg dm^{-3} ATMP concentration.

Figure 8 displays chronoelectrogravimetric curves for various ATMP concentrations: the mass of scale deposited after a given time decreased when ATMP concentration increased (e.g., it was less than 2 μg cm^{-2} after 80 min for a 0.4 mg dm^{-3} ATMP concentration). They show that the scaling time increased when ATMP concentration increased and that the mass plateau was never reached during the time of

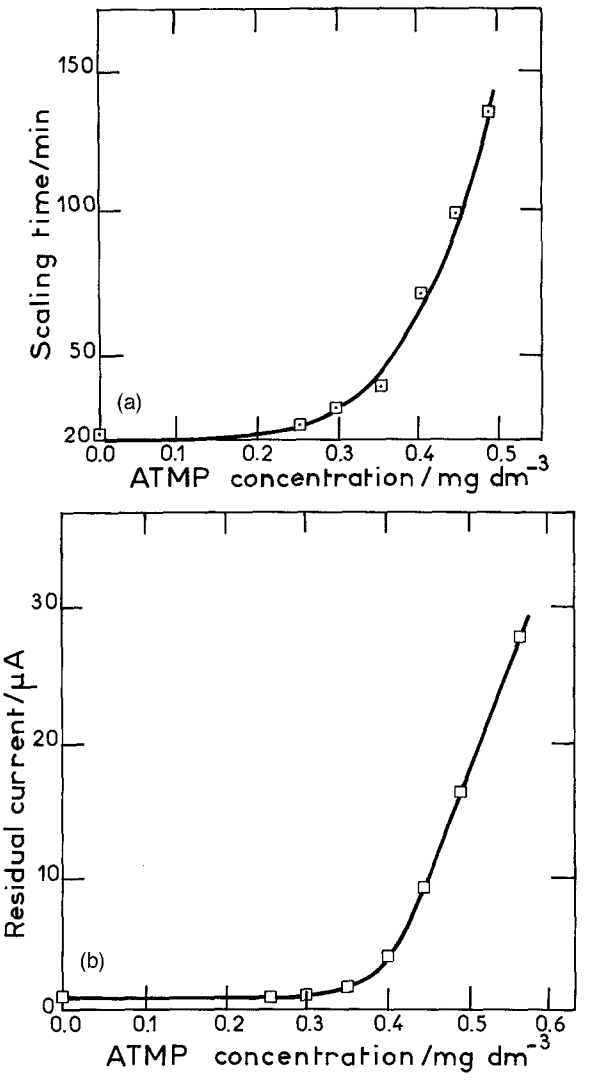

Fig. 7. Scaling parameters deduced from chronoamperometric curves against ATMP concentration. (a) Scaling time. (b) residual current.

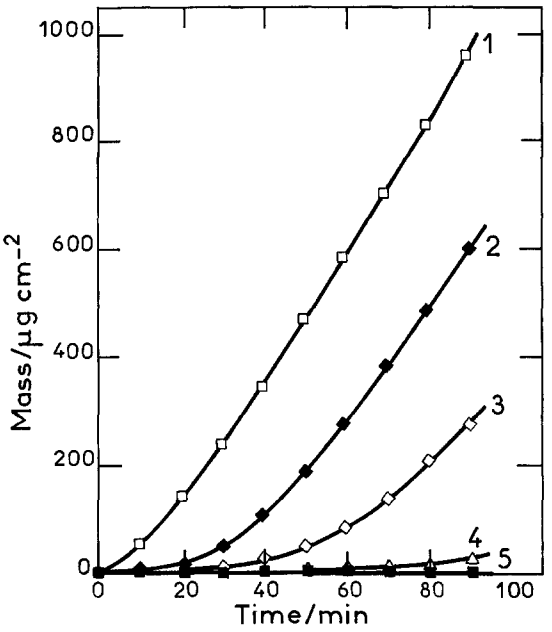

Fig. 8. Chronoelectrogravimetric curves plotted for various ATMP concentrations. (1) No addition; (2) 0.25, (3) 0.3, (4) 0.35 and (5) 0.6 mg dm^{-3}.

the experiment (90 min). The linear part is not always visible, however, it may be supposed that all the curves are parallel in the intermediate region. Therefore, it was not the scaling rate which decreased with the phosphonate concentration but rather the nucleation time which increased.

The impedance was measured after 3 h of $CaCO_3$ deposition (which is a time sufficient to totally cover the electrode for water without ATMP). As soon as 0.1 mg dm^{-3} of ATMP was added, the diffusion loop observed for water with no ATMP disappeared (Fig. 9(a)). Only the half circular loop remained whose diameter regularly diminished with ATMP concentration (Fig. 9(b)). This shows that, when ATMP was added, the electrode surface was not totally covered by scale even after 3 h.

The electrode surface was examined using scanning electron microscopy (SEM) with various magnifications. The pictures obtained are given in Fig. 10 for water without and with 0.6 mg dm^{-3} ATMP. For water without ATMP, the electrode is entirely covered by a $CaCO_3$ deposit. Entangled rhombohedrons with sharp edges, characteristic of calcite, were particularly visible with a high magnification. When ATMP was added only very tiny nuclei on aggregates of $CaCO_3$ with amorphous aspect were observable. No trace of crystallization was observed and the electrode surface was almost totally bare. Only a few small zones covered by $CaCO_3$ were observed using SEM.

4.3. *Polyacrylates*

These macromolecules are used in water treatments as flocculating agents, they also have some antiscale properties. The efficiency of P3 Ferrofos 5248 (Henkel) was tested in natural waters. When polyacrylate concentration increased from 0.3 to 6 ppm,

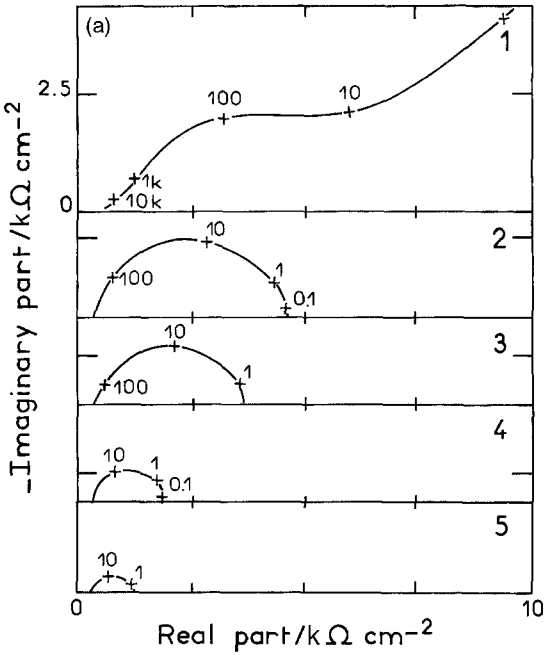

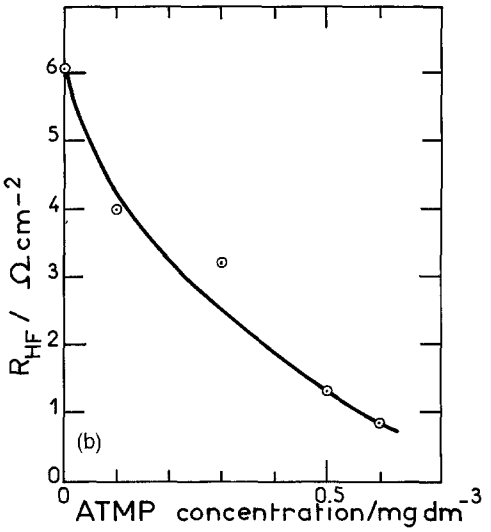

Fig. 9. (a) Measured electrochemical impedances after 3 h of scale deposition for various ATMP concentration. (1) No addition; (2) 0.1, (3) 0.3, (4) 0.5 and (5) 0.6 mg dm^{-3}. (b) Change of R_{HF} against ATMP concentrations.

chronoamperometric curves showed an increase in both the scaling time and the residual current (Fig. 11).

Tests by chronoelectrogravimetry in natural waters showed that 80 μg of scale was deposited after 30 min. In contrast, when a minute quantity of polyacrylate (0.3 mg dm^{-3}) was added only 0.3 μg was deposited in the same time (Fig. 12). Scaling was much lower as the inhibitor quantity increased, from 6 mg dm^{-3} concentration, no more deposit was observed (i.e., it was lower than 20 mg which was the sensitivity of the microbalance used).

5. Conclusion

The efficiency of chemical antiscale treatments was assessed by various techniques: chronoamperometry, chronoelectrogravimetry and impedance measurement. Similar results were obtained but electrogravimetry

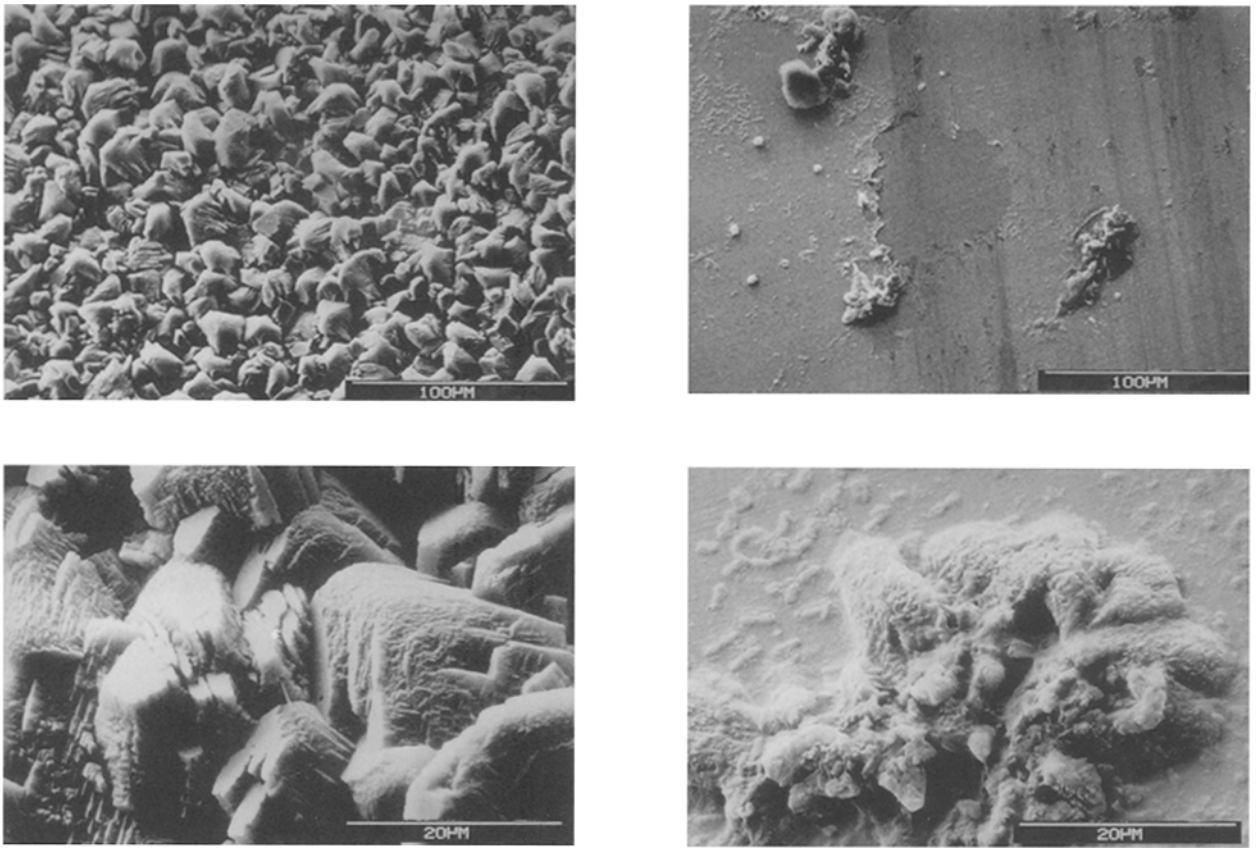

Fig. 10. Observations of a $CaCO_3$ deposition with (right) and without (left) addition of 0.6 mg dm^{-3} ATMP at two magnifications.

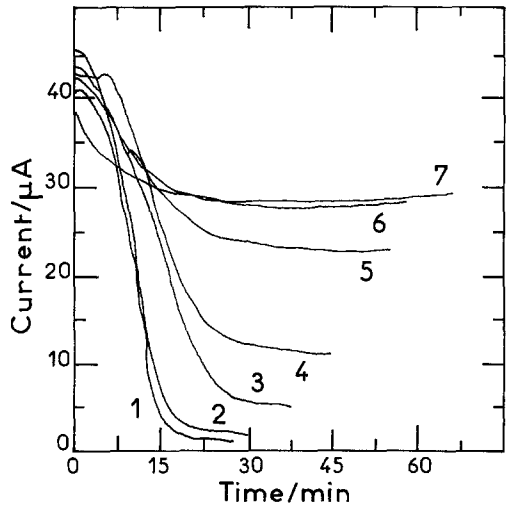

Fig. 11. Chronoamperometric curves obtained with various Ferrofos concentrations: (1) No addition; (2) 0.3, (3) 1, (4) 2, (5) 3, (6) 4 and (7) 6 mg dm^{-3}.

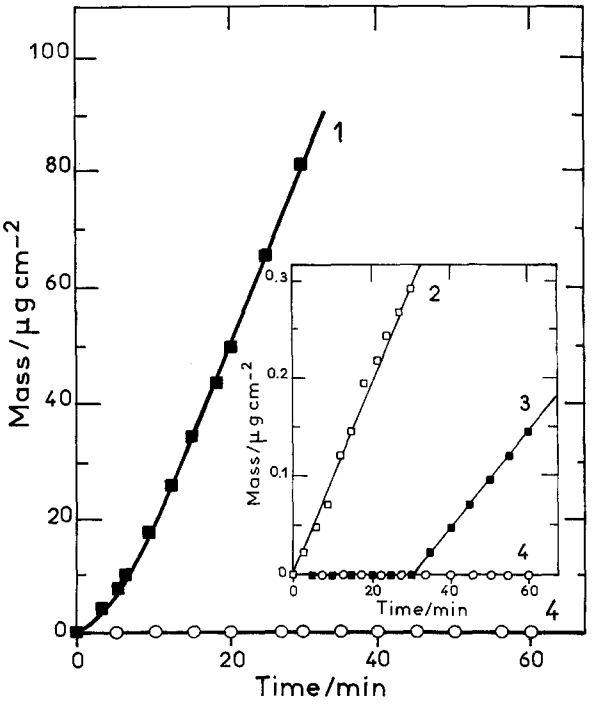

Fig. 12. Chronoelectrogravimetric curves obtained with various Ferrofos concentrations: (1) No addition; (2) 0.3, (3) 2 and (4) 6 mg dm^{-3}.

gave data directly readable by the user. The particular chemistry of the additives may give results more difficult to interpret through chronoamperometry where the residual current often increases when the quantity of antiscale chemical species increases.

References

[1] L. Legrand, G. Poirier and P. Leroy, Les équilibres carboniques et l'équilibre calcocarbonique dans les eaux naturelles, Eyrolles, Paris (1981).

[2] H. Roques, Fondements théoriques du traitement chimique des eaux, Vols I and II, Techniques de documentation, Lavoisier, Paris (1990).

[3] J. Ledion, P. Leroy and J.-P. Labbé, *TSM L'eau*, July/Aug., (1985).

[4] W. Lin, C. Colin and R. Rosset, *TSM L'eau*, Dec. (1990).

[5] P. Leroy, W. Lin, J. Ledion and A. Khalil, *J. Water SRT, Aqua.* **42**(1) (1993) 23.
[6] A. Khalil, R. Rosset, C. Gabrielli, M. Keddam and H. Perrot, *J. Appl. Electrochem.*, (to be published).
[7] S. Bourkane, C. Gabrielli and M. Keddam, *Electrochim. Acta* **34** (1989) 1081.
[8] V. Bouet, C. Gabrielli, G. Maurin and H. Takenouti, *J. Electroanal. Chem.* **340** (1992) 325.
[9] A. Khalil, P. Sassiat, C. Colin, C. Meignen, C. Garnier, C. Gabrielli, M. Keddam and R. Rosset, *C.R. Acad. Sci. Paris*, **314** sér. II (1992) 145.
[10] C. Gabrielli, M. Keddam, A. Khalil, G. Maurin, R. Rosset and M. Zidoune, *J. Electrochem. Soc.*, (to be published).
[11] A. Khalil, C. Colin, C. Gabrielli, M. Keddam and R. Rosset, *C.R. Acad. Sci. Paris*, **316** sér. II (1993) 19.
[12] C. Gabrielli, M. Keddam, A. Khalil, R. Rosset and M. Zidoune, *Electrochim. Acta*, (to be published).
[13] C. Deslouis, C. Gabrielli, M. Keddam, A. Khalil, R. Rosset, B. Tribollet and M. Zidoune, *Electrochim. Acta*, (to be published).
[14] F. Hui. P. Garcia-Camacho and R. Rosset, *Analysis* **23** (1995) 58.
[15] Bulletin technique Monsanto 53–46 (F) ME-1, Les séries des phosphonates, Dequest 2000 et 2010 (1988).
[16] M. Zidoune, A. Khalil, P. Sakyat, C. Colin and R. Rosset, *C.R. Acad. Sci. Paris*, **315** sér. II (1992) 795.